Food Chemistry: X 14 (2022) 100282

Contents lists available at ScienceDirect

Food Chemistry: X

journal homepage: www.sciencedirect.com/journal/food-chemistry-x

Physicochemical and antioxidant properties of *Lycium barbarum* seed dreg polysaccharides prepared by continuous extraction

Xiu-Xiu Zhang [a], Zhi-Jing Ni [b], Fan Zhang [a], Kiran Thakur [a,b], Jian-Guo Zhang [a,b], Mohammad Rizwan Khan [c], Rosa Busquets [d], Zhao-Jun Wei [a,b,*]

[a] School of Food and Biological Engineering, Hefei University of Technology, Hefei 230009, People's Republic of China
[b] School of Biological Science and Engineering, North Minzu University, Yinchuan 750021, People's Republic of China
[c] Department of Chemistry, College of Science, King Saud University, Riyadh 11451, Saudi Arabia
[d] School of Life Sciences, Pharmacy and Chemistry, Kingston University London, Kingston Upon Thames, KT1 2EE Surrey, England, United Kingdom

ARTICLE INFO

Keywords:
Lycium barbarum seed dreg
Polysaccharides
Continuous extraction
Physicochemical
Anti-oxidant
Functional properties

ABSTRACT

Lycium barbarum seed dreg polysaccharides (LBSDPs) were continuously extracted with four different solvents [hot buffer (HBSS), chelating agent (CHSS), dilute alkaline (DASS), and concentrated alkaline (CASS)]. The present study characterized the physicochemical and anti-oxidant based functional properties of different LBSDPs. The monosaccharide analysis revealed xylose (64.63%, 70.00%, 44.71%, and 66.67%) as the main sugar with the molecular weights of 5985, 7062, 5962, and 8762 Da in HBSS, CHSS, DASS, and CASS, respectively. Among the four polysaccharides, CASS had the strongest DPPH radical scavenging ability and reducing power; while, CHSS had the strongest ferrous ions chelating ability and HBSS showed the strongest OH radical scavenging ability. In terms of functional properties, HBSS and CASS had better solubility and oil holding capacity, while, CASS and CHSS had higher foam capacity and foam stability. Altogether, the polysaccharides extracted from *L. barbarum* seed dreg exhibit a potential application prospect in functional food and cosmetics industries.

Introduction

Lycium barbarum, a plant of the Solanaceae family, is a valuable herbal medicine, rich in amino acids, proteins, carotenoids, flavonoids, betaine, taurine and vitamins, which nourishes the liver and kidney (Kulczyński, & Gramza-Michałowska, 2016). *L. barbarum* polysaccharide (LBP) is the main active ingredient of Wolfberry, endowed with different biological activities, such as anti-tumors (Wang et al., 2020), immunomodulation (Liu et al., 2022), regulation of blood sugar and lipid metabolism (Yang et al., 2021), improvement of osteoporosis (Wang et al., 2019), and anti-radiation (Zheng et al., 2021). Due to its rich flavor, *L. barbarum* has become a key research plant in the food and pharmaceutical industries (Kulczyński, & Gramza-Michałowska, 2016). Since time immortal, *L. barbarum* has been used as a food ingredient as well active medicinal compound in China. An enormous annual yield and consumption of *L. barbarum* have been reported in China, ranking first in the world (Mascia et al., 2018). With the rapid increase in the development of Goji based processed food products, a huge amount of by-product *L. barbarum* seed dreg (LBSD) is generated which causes a considerable environmental and health concern (Long et al., 2020). Despite its rich nutrition, the full potential of LBSD still remains unfathomed (Li et al., 2011).

Polysaccharides extracted from plants are a class of biomolecular compounds consisting of different monosaccharides linked by α or β glycosidic bonds through the substitution of hydroxyl hydrogens on hemiacetal groups (Xie et al., 2016). Modern pharmacological evidence showed the anti-tumors, anti-bacterial, anti-viral, immunomodulatory, antioxidant and other biological activities of polysaccharides (Yu, Shen, Song, & Xie, 2018; Chen et al., 2022; Xie et al., 2022). Although the biological activity of LBP is of great interest, the structure of LBP is complex and these polysaccharides cannot be synthesized artificially, and they cannot be easily extracted (Wang et al., 2019). In the recent years, the search for efficient extraction methods without destroying the structure of LBP is an eminent area of research (Yuan, Nie, Liu, & Ren, 2021). At present, their extraction methods mainly include water extraction and alcohol precipitation method, ultrasonic assisted method,

Abbreviations: LBP, *Lycium barbarum* polysaccharide; LBSD, *Lycium barbarum* seed dreg; LBSDP, *Lycium barbarum* seed dreg polysaccharide.

* Corresponding author at: School of Food and Biological Engineering, Hefei University of Technology, Hefei 230009, People's Republic of China.
E-mail addresses: zffs2012@mail.ahnu.edu.cn (F. Zhang), kumarikiran@hfut.edu.cn (K. Thakur), zhangjianguo@hfut.edu.cn (J.-G. Zhang), mrkhan@KSU.EDU.SA (M.R. Khan), r.busquets@kingston.ac.uk (R. Busquets), zjwei@hfut.edu.cn (Z.-J. Wei).

https://doi.org/10.1016/j.fochx.2022.100282
Received 6 February 2022; Received in revised form 28 February 2022; Accepted 7 March 2022
Available online 10 March 2022

microwave method, and enzymatic digestion method (Yuan et al., 2022). In previous studies, four different solutions (hot buffer, chelating agent, dilute alkaline, and concentrated alkaline) have been commonly used to obtain four different polysaccharides from okara (Sengkhamparn et al., 2009), onion (Ma et al., 2018), potato peel (Xu et al., 2019), *Amana edulis* (Ji et al., 2019) and peony seed dreg (Li et al., 2018) by sequential extraction method. These fractions showed distinct differences in chemical composition, anti-oxidant activity, and antibacterial properties. So far, there are no reports on polysaccharides sequentially extracted from *L. barbarum* sees dreg. Hence, it makes our study valuable to offer the necessary contributions for *L. barbarum* seed dreg derived polysaccharides.

In present study, *L. barbarum* seed dreg polysaccharides (LBSDPs) were sequentially extracted by four different solutions and represented by qualitative and quantitative analysis, including UV in the range of 200–800 nm, FT-IR between 4000 and 400 cm^{-1}, GC for detection of monosaccharide composition, molecular weight determination, and characterization of chemical composition (total sugar, protein, and uronic acid). We also determined the antioxidant activities (ABTS radical, DPPH radical, OH radical scavenging, and Fe^{2+} chelating activities) and functional characteristics of the polysaccharides.

Materials and methods

Materials and chemicals

L. barbarum seed dreg (LBSD), as a byproduct of *L. barbarum* seed was obtained after oil extractions from Ningxia Wolfberry Goji Industry Co., Ltd (Yinchuan, China). Because of insignificant oil content, LBSD was directly passed through a screen (60-mesh) without degreasing. The obtained LBSDs were sealed and stored in −20 °C. Reagents like phenol, EDTA-2Na, and $NaBH_4$ were all of analytical grade.

Continuous extraction of LBSDPs

The obtained LBSD was obtained after magnetic stirring with 70% ethanol for 2 h and the insoluble solid obtained by suction filtration was washed with chloroform/methanol (1/1, v/v) followed by filtration. The filtered residue was washed with acetone and then filtered (Sengkhamparn et al., 2009). The powder (AIS) was placed in a cool and ventilated place for air drying, sealed and stored in a 4 °C refrigerator for subsequent experiments.

Further, 20 g of LBSD-AIS was added to 600 mL 0.05 mol/L pH 5.2 CH_3COONa solution and allowed to react in a constant temperature water bath at 70 °C for 1 h. After suction filtration, HBSS was the filtrate product of the first stage. The filtered residue was added to 0.05 mol/L $(NH_4)_2C_2O_4$, CH_3COONa, and EDTA-2Na pH 5.2 solution. After reacting in a 70 °C water bath for 1 h, the solid and liquid were separated. CHSS was the liquid product of the second stage. The solid was then added to 0.05 mol/L NaOH and 20 mmol/L $NaBH_4$ solution. After reacting in a 4 °C refrigerator for 1 h, the above operations were repeated. DASS was the liquid product of the third stage. Then solid product was added to 5 mol/L NaOH and 20 mmol/L $NaBH_4$ solution and allowed to react at 4 °C for 2 h followed by centrifugation at 7155 *g* for 15 min, and the supernatant (CASS) was obtained as the product of fourth stage (Ji et al., 2019). After deproteinization by Sevage reagent (Long et al., 2020), the four products were dialyzed at 4 °C for 2 d, and the distilled water was changed regularly to ensure the internal and external osmotic pressure before the full dialysis. The dialyzed solutions were concentrated, precooled, and freeze-dried (Sengkhamparn et al., 2009).

Infrared spectroscopy of LBSDPs

The functional groups of the four fractions were characterized by Fourier transform infrared spectroscopy (Spectrum Two, Perkin Elmer, Waltham, USA). Briefly, a certain amount of dried polysaccharide samples was pressed with KBr, and scanned under the wavelength range of 4000–400 cm^{-1} (Ji et al., 2019).

UV absorption peak detection

The LBSD polysaccharides were prepared into 1 mg/mL, then UV full band scanning was carried out in the range of 200–800 nm (Li et al., 2018).

LBSDPs composition analysis

According to phenol–sulfuric acid method (Xu et al., 2019), the standard curve was obtained by gradient concentration glucose solution ($y = 0.2404x - 0.0172$, x: glucose concentration (μg/mL) and y: A_{490nm}, $R^2 = 0.9936$). The uronic acid content in the four different fractions was quantified by M-hydroxybiphenyl method (Ji et al., 2019), in which galacturonic acid was used as the control. The standard curve of galacturonic acid series gradient was obtained as $y = 0.0033x + 0.0706$, x: uronic acid concentration (μg/mL), y: A_{520nm}, $R^2 = 0.9945$. The protein content was determined by Coomassie protein assay kit ($y = 0.4153x + 0.635$, x: protein concentration (mg/mL), y: A_{595nm}, $R^2 = 0.9990$) (Ma et al., 2018).

Detection of thermal properties

The thermal properties of LBSD polysaccharide powder were measured by differential scanning calorimeter Q200 (TA Instruments, New Castle, USA). For this, 4 mg of dried polysaccharide powder was added into the aluminum crucible and sealed under pressure. On the other hand, the empty crucible was taken as the control. The temperature was increased from 20 °C to 250 °C at a rate of 10 °C/min. N_2 was used as the carrier gas at the flow rate of 50 mL/min (Ji et al., 2019).

Analysis of monosaccharide compositions

Briefly, the four polysaccharides were acetylated after hydrolysis, and gas phase analysis was carried out after passing through the membrane of 0.22 μm (Tianjin Jinteng Experimental Equipment Co., Ltd, Tianjin, China). The mixed standard was composed of six different monosaccharides standards (Xu et al., 2019).

Determination of molecular weight of LBSDPs

According to high performance gel permeation chromatography (HPGPC) (LC-10A, Shimadzu), LBSDPs (2 mg/mL) were filtered through 0.22 μm filter membrane (Tianjin Jinteng Experimental Equipment Co., Ltd, Tianjin, China). Referring to the calibration curve of dextran series standard solutions, the molecular weights of four polysaccharides (LBSDPs) were determined. Chromatographic conditions: column: BRT105-104-102 tandem gel column (8 × 300 mm); mobile phase: 0.05 M NaCl solution; and detector: RI-10A differential detector at 40 °C with a flow rate of 0.6 mL/min and injection volume of 20 μL (Tang et al., 2020).

Field emission scanning electron microscope

The small amounts of different polysaccharide fractions were scattered on a tape which was adhered to the aluminum plate. After carefully blowing off the excess polysaccharide with an ear washing ball, it was gold coated to make the sample conductive and observed with a high-resolution field emission electron scanning microscope (Hitachi, Regulus 8230, Tokyo, Japan) (Ma et al., 2018). HBSS was examined at magnification (1000× and 5000×), CHSS at magnification (1000× and 10 k×), DASS at magnification (1000× and 2000×), and CASS at magnification (1000× and 2000×).

Functional characterizations of LBSDPs

Solubility

The dried LBSD polysaccharide powder (100 mg) was poured into a centrifuge tube and the overall weight was recorded as W_0. Then, 10 mL of deionized water was poured into a tube and the obtained suspension was stirred at 75 r/min for 90 min at 25 °C and centrifuged at 6,000 rpm for 15 min. After pouring out the supernatant, the tubes were dried in an oven at 60 °C for 30 min and the weight was recorded as W_1 (Xu et al., 2019). The solubility was calculated as:

$$Solubility\,(\%) = \frac{W_0 - W_1}{W_0} \times 100 \quad (1)$$

Fat-binding ability

The dried LBSD polysaccharide powder (500 mg) was poured into a centrifuge tube and the total weight was recorded as W_0. Then corn oil (10 mL) was poured into the tube and shaken evenly at the speed of 75 r/min for 90 min. The resulting blend was centrifuged at 6000 rpm for 15 min and dried at 60 °C for 30 min. The total weight was recorded as W_1 (Xu et al., 2019). The fat-binding capacity was calculated as:

$$Fat-binding\ capacity\ (\%) = \frac{W_0 - W_1}{W_0} \times 100 \quad (2)$$

Foam capacity and foam stability

The LBSD polysaccharide powder (20 mg) was mixed with 10 mL of distilled water and the volume was determined as V_0. Then obtained suspension was.

homogenized at 10,000 rpm for 3 min with a high-speed shearing machine (IKA-T25 digital Ultra-Turrax, Selangor, Malaysia) and the volume was measured as V_T after 30 min (Ji et al., 2019). The foam capacity and foam stability were calculated as:

$$Foam\ capacity\,(\%) = \frac{V_t - V_0}{V_0} \times 100 \quad (3)$$

$$Foam\ stability\,(\%) = \frac{V_T - V_0}{V_0} \times 100 \quad (4)$$

Antioxidant activity

ABTS radical scavenging activity

ABTS radical stock solution was prepared by mixing reagent A (0.0384 g ABTS constant volume to 10 mL) and reagent B (0.0134 g $K_2S_2O_8$ constant volume to 10 mL) in equal volumes and stored at room temperature without direct light exposure and diluted until its absorbance at 734 nm reached about 0.68–0.72. The freshly prepared ABTS working solution was stored without direct light exposure. Then, a series of gradient concentration polysaccharide solutions (0.1, 0.2, 0.4, 0.6, 0.8, 1.0, 2.0, 3.0, 4.0, and 5.0 mg/mL) was prepared using distilled water; and 4 mL of ABTS solution was poured into 200 μL of each LBSDP fraction. The resulting blend was gently shaken and stored at 25 °C for 6 min followed by absorbance measurement at 734 nm (A_1) with enzyme labeling instrument (Epoch™, Biotek, Vermont, USA). The same concentrations of V_C were treated in the same way and taken as the positive control (A_0), and distilled water was treated as the blank control (A_2) (Li et al., 2018). The ABTS radical scavenging ability was calculated as follow:

$$ABTS\ radical\ scavenging\ activity\,(\%) = \frac{A_0 - A_1 + A_2}{A_0} \times 100 \quad (5)$$

DPPH radical scavenging activity

The series of gradient concentrations of LBSD polysaccharide aqueous solutions were prepared in the same way as mentioned in Section "ABTS radical scavenging activity". 2 mL of 0.1 mmol/L DPPH methanol solution was poured into an equal volume of each LBSD polysaccharide solution. The resulting blend was mixed and stored at 25 °C for 30 min. Further, 200 μL of final reaction solution was added into 96 well plate for absorbance (517 nm) measurement (A_1). The same concentrations of V_C were treated in the same way and taken as the positive control (A_0) at 517 nm. 2 mL of distilled water was added into each polysaccharide solution, and the absorbance was determined as A_2 (Ji et al., 2019). The DPPH radical scavenging ability was calculated as follow:

$$DPPH\ radical\ scavenging\ activity\,(\%) = \frac{A_0 - A_1 + A_2}{A_0} \times 100 \quad (6)$$

OH radical scavenging activity

For this, 1 mL of 9 mM $FeSO_4$ solution was firstly poured into an equal volume of LBSD polysaccharide solution and then an equal volume of 9 mM salicylic acid was poured into the blending solution. Further, 1/2 vol of 0.1% H_2O_2 was added into the resulting mixture. The resulting blend was reacted in a water bath at 37 °C for 30 min and the absorbance measured at 510 nm was considered as A_1. The same concentrations of V_C were taken as the positive control (A_0) and the absorbance (A_2) was obtained by adding 2.5 mL pure water to polysaccharide solutions with different concentrations under the same conditions (Li et al., 2018). The OH radical scavenging activity was calculated as follow:

$$OH\ radical\ scavenging\ activity\,(\%) = \frac{A_0 - A_1 + A_2}{A_0} \times 100 \quad (7)$$

Fe^{2+} chelating activity

For this, 0.1 mL of 2 mM $FeCl_2$ solution was poured into 1 mL of LBSD polysaccharide solution of different concentrations followed by the addition of 0.2 mL of 5 mM phenanthroline. Further, 2.7 mL of pure water was poured into the reaction solution and the resulting blend was reacted at 25 °C for 10 min. The absorbance measured at 562 nm was recorded as A_1. The polysaccharide solution was replaced with pure water and treated under the same conditions, and the absorbance obtained was recorded as A_0. The absorbance obtained after adding 3 mL of pure water to the polysaccharide solution was recorded as A_2. The EDTA-2Na was used as the positive control (Li et al., 2018). The Fe^{2+} chelating activity was calculated as follow:

$$Fe^{2+}\ chelating\ activity\,(\%) = \frac{A_0 - A_1 + A_2}{A_0} \times 100 \quad (8)$$

Total antioxidant capacity

For this, 2.5 mL of 0.2 M PBS and 1% $K_3Fe(CN)_6$ were successively poured into 1 mL of different polysaccharide concentrations. After the resulting blend was allowed to react in a water bath at 50 °C for 20 min, 2.5 mL of 10% TCA was poured into the solution. The resulting solution was centrifuged at 7155 g for 15 min and 2 mL of pure water was added into 2.5 mL of supernatant. Further, 1 mL of 0.1% $FeCl_3$ was poured into the resulting blend for absorbance measurements (A_{700} nm) (Ji et al., 2019).

Statistical analysis

The mean ± standard deviations were used for statistical comparison of the multiple groups using one-way ANOVA through SPSS 21.0 at $P < 0.05$. One way ANOVA was used for inter group comparison, and origin 8.0 software was used for graphs.

Results and discussion

Chemical compositions of LBSDPs

The chemical composition of LBSDPs showed that the extractions yield of HBSS, CHSS, DASS, and CASS were 4.76%, 2.79%, 4.35%, and 5.6%, respectively (Table 1). The four different polysaccharides did not

Table 1
Chemical composition, the molecular weight and monosaccharide composition of different polysaccharides extracted from *L. barbarum* seed dreg. Values were expressed as mean ± SD of three replicates.

Index	Samples			
	HBSS	CHSS	DASS	CASS
Extraction yield (%)	4.76 ± 0.33	2.79 ± 0.77	4.35 ± 0.30	5.60 ± 0.38
Total sugar (%)	86.26 ± 0.74	82.59 ± 4.93	83.32 ± 0.66	84.45 ± 1.87
Uronic acid (%)	0.69 ± 0.04	0.79 ± 0.03	0.10 ± 0.04	0.41 ± 0.06
Protein (%)	0.42 ± 0.02	0.80 ± 0.08	3.43 ± 0.08	2.46 ± 0.06
Molecular weights (Da)				
Mw	5985	7062	5962	8762
Mn	3661	5463	4647	6609
Mw/Mn	1.63	1.29	1.28	1.33
Monosaccharide components (%)				
Rha	15.34	12.59	9.39	17.23
Xly	64.63	70.00	44.71	66.67
Ara	4.48	4.68	2.84	4.55
Gal	9.35	9.93	6.27	9.75
Man	4.87	1.49	35.04	0.68
Glc	1.75	1.31	1.76	1.11

show significant difference in the total sugar content (80%). Among all the fractions, HBSS amounted for 86.26%, indicating that sugar was the main chemical component in different polysaccharide samples. Protein and uronic acid represented the minor amount in four polysaccharides, which was like that of okra polysaccharides (Sengkhamparn et al., 2009).

FT-IR analysis

As shown in Fig. 1A, the infrared spectra of LBSDPs revealed some of the functional groups and glycosidic bonds in the range of 4000–400 cm^{-1}. The infrared spectra could reveal whether there were any differences in the structure of four LBSD polysaccharides. From the Fig. 1A, it can be observed that the infrared spectra of the four different polysaccharides fractions were relatively similar. The two characteristic absorption peaks of polysaccharides were observed as the O—H stretching vibration around 3400 cm^{-1} and the C—H stretching vibration near 2900 cm^{-1} (Al-Sheraji et al., 2012, Li et al., 2014). Four LBSD polysaccharides showed absorption peaks of intensity near 3400 cm^{-1} and 2900 cm^{-1}. The characteristic peaks for HBSS, CHSS, DASS, and CASS at 1649, 1586, 1620, and 1575 cm^{-1} represented their protein content which was consistent with previous study that reported the stretching bands at 1650 and 1550 cm^{-1} (Abuduwaili et al., 2022). The peaks at 1408 cm^{-1} (HBSS), 1404 cm^{-1} (CHSS), 1396 cm^{-1} (DASS), and 1403 cm^{-1}(CASS) were related to the existence of C═O bond, which indicated the presence of uronic acid (Cui et al., 2016, Liu et al., 2017). The absorption peaks at 1052 cm^{-1} for HBSS, 1077 cm^{-1} for CHSS, 1047 cm^{-1} for DASS and 1077 cm^{-1} for CASS were attributed to C—O vibration (Luo et al., 2010). Whereas, there was a slight difference among the four LBSD polysaccharides in the glycosidic linkages. The absorption peak at 890 cm^{-1} indicated a β-glycosidic bond and the absorption peak at 830 cm^{-1} indicated an α-glycosidic bond (Liu et al., 2022, Fang, Chen, & Kan, 2020). HBSS and CHSS showed the absorption peaks at 850 and 857 cm^{-1}, respectively, which represented the β-glycosidic bond chain linkage in their sugar units, while DASS and CASS at 833 and 832 cm^{-1} were assigned to α-glycosidic bond, respectively.

UV absorption peak analysis

The UV spectra of four different polysaccharides fractions had relatively concentrated maximum absorption peaks, implying that the polysaccharide composition was relatively homogeneous (Fig. 1B) (Abuduwaili et al., 2022). The wavelengths corresponding to the maximum absorption peaks were 214, 210, 208, and 216 nm, respectively, which might be due to their slightly different internal structures (Sengkhamparn et al., 2009). The four fractions had tiny absorption peaks in the range of 250–280 nm, and previous studies have shown that band between 250 and 300 nm corresponds to electronic transition of –CO-NH- (Li et al., 2020). Our results showed that the four different polysaccharides had relatively high purity compared to the previous reported study on *Dictyophora indusiata* polysaccharides (Liu et al., 2017).

DSC analysis

The DSC curves are based on the vertical coordinate of heat flow rate (W/g) and the horizontal coordinate of the temperature (°C) or time (t), which can measure a variety of thermodynamic and kinetic parameters, such as sample purity, crystallization rate, and heat of reaction (Bellich et al., 2015). The thermal characteristics of HBSS, CHSS, DASS, and CASS were demonstrated by DSC as shown in Fig. 2 which determined that LBSDPs had peaks in the range of 25–250 °C. The peaks for four LBSDPs were 72.42–156.94 °C, 93.49–201.41 °C, 91.95–166.30 °C, and 109.07–185.37 °C, respectively. It can be related with the structural

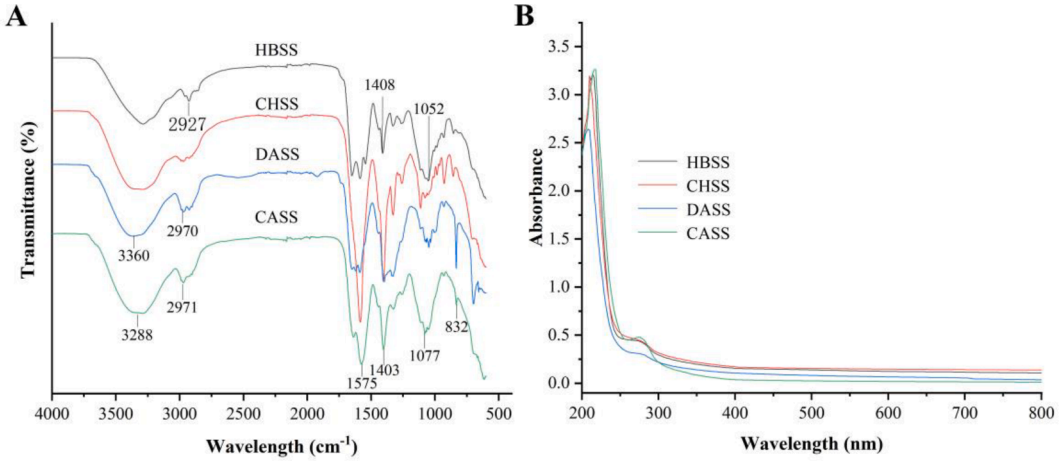

Fig. 1. FT-IR spectrometric analysis of LBSDPs within the frequency range of 4000–400 cm^{-1} (A). UV spectra of LBSDPs within the wavelength range of 190–800 nm (B).

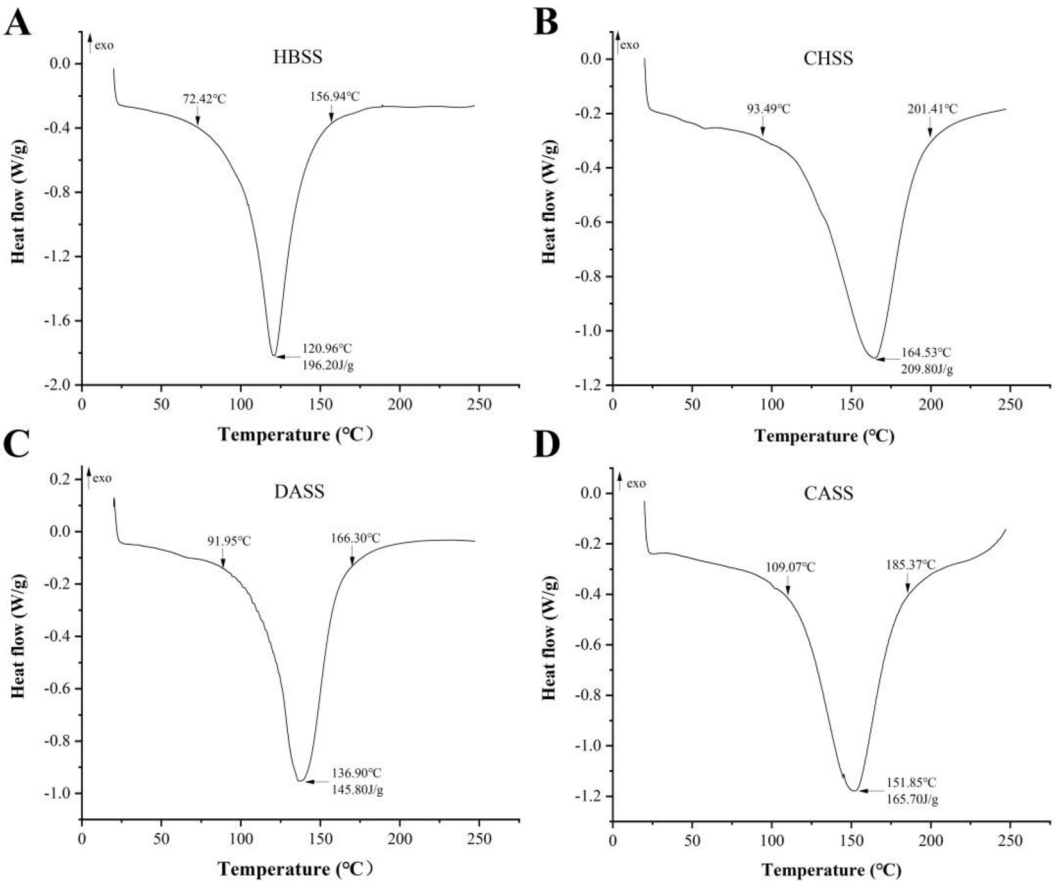

Fig. 2. The DSC properties of LBSDPs. (A) HBSS, (B) CHSS, (C) DASS, (D) CASS.

difference between the polysaccharides as reported in the previous studies (Xu et al., 2019, Iijima, Hatakeyama, & Hatakeyama, 2012). Previous studies confirmed that with the wider temperature range, the thermal stability of the substance was lowered (Xu et al., 2019, Ji et al., 2019). For four different fractions, the peak temperatures were observed at 120.96 °C, 164.53 °C, 136.9 °C, and 151.85 °C, respectively. The total thermal energy values of HBSS, CHSS, DASS, and CASS per unit mass were 196.20 J, 209.80 J, 145.80 J, and 165.70 J, respectively. The ΔH can be corresponded with hydrogen bonds in a substance (Li et al., 2014). It was noticed that CHSS had the largest ΔH and temperature range. Hence, CHSS had the highest thermal stability, which can be applied to baking industry to improve the texture of baked goods (Hirai et al., 2012).

Monosaccharide composition and molecular weight analysis

According to GC–MS data (Table 1), the retention times of rhamnose, arabinose, xylose, mannose, glucose, and galactose were 17.7, 18.0, 18.7, 20.2, 20.4, and 20.5 min, respectively. HBSS consisted of six monosaccharides – Rha, Xyl, Ara, Gal, Glc, and Man with the percentages of 15.34, 64.53, 4.38, 9.15, 4.85, and 1.75%, respectively. Likewise, CHSS consisted of 12.59, 70.00, 4.68, 9.93, 1.49, and 1.31%, respectively. DASS consisted of 9.93, 44.71, 2.83, 6.27, 35.04, and 1.76%, respectively. CASS comprised of six monosaccharides with the percentages of 17.23, 66.67, 4.55, 9.75, 0.68, and 1.12%, respectively. HBSS mostly consisted of Xyl (>60%), while, DASS mainly consisted of Xyl (44.71%) and Gal (35.04%).

Based on the HPGPC, the molecular weight of LBSD polysaccharides was characterized by weight average, number average molecular weight, and polydispersity index, as exhibited in Table 1. The standard curve of dextran with different molecular weight was LgMw-RT correction curve: $y = -0.2056x + 12.69$ (x: retention time, $R^2 = 0.9948$). The structural and functional properties of polysaccharides were related to their molecular weights (Ji et al., 2019). The Mws of four LBSDPs were 5985 Da, 7062 Da, 5962 Da, and 8762 Da. The Mw/Mn values were 1.63, 1.29, 1.28, and 1.33, respectively. Our results indicated that the difference of molecular weights of HBSS, CHSS, DASS and CASS may be caused by different extraction solvents.

Morphological characteristics of extracted polysaccharides

The surface morphology of HBSS, CHSS, DASS, and CASS of the four different LBSDPs was represented in Fig. 3. The microscopic phenotypes of all the four polysaccharides showed the characteristic structure of polysaccharides, in the form of flakes or rods, but there were differences in the specific phenotypes. HBSS showed typical flat flakes, mostly curved with good malleability. CHSS had a loose and porous surface, with a large surface area and many active binding sites. DASS showed relatively aggregated rods when observed at high magnification, the reason for this phenomenon may be the existence of hydrogen bonds within and between molecules of DASS, which leads to aggregation (Tan, Zhao, & Zhao, 2021). DASS showed spherical particles on the molecular surface, probably starch granules or proteins (Sengkhamparn et al., 2009). This characteristic surface suggested that the fluidity of polysaccharide was passable (Tan, Zhao, & Zhao, 2021). CASS showed typical rods, with intermolecular aggregation, and good malleability. Different extraction solutions and the continuity of extraction may lead to the changes of chemical bonds within and between the four LBSD polysaccharides, resulting in the difference of micro morphological structure (Xu et al., 2019).

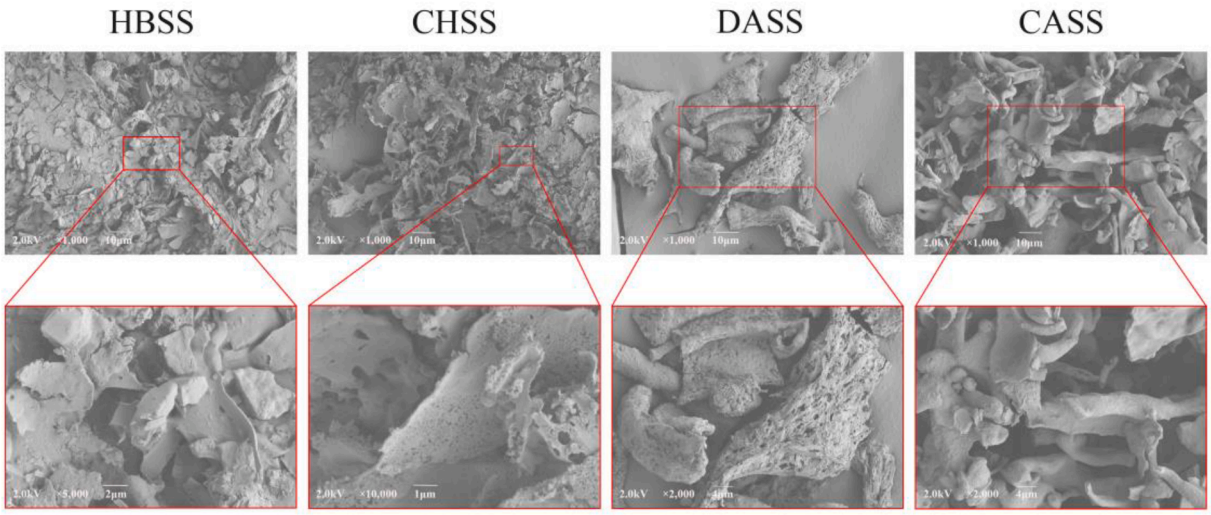

Fig. 3. Field emission scanning electron micrographs of LBSDPs. HBSS at magnification (1000× and 5000×), CHSS at magnification (1000× and 10 k×), DASS at magnification (1000× and 2000×), and CASS at magnification (1000× and 2000×).

Functional characterizations

The functional characteristics of LBSDPs are shown in Fig. 4. HBSS and CASS showed similar solubility; while, CASS had the highest solubility among the four components, up to 97.9%, which was related to the lower extent of branching as compared to remaining fractions (Kan, Chen, Zhou, & Zeng, 2021). The fat-binding ability of the four LBSDPs was represented as 3.16, 2.25, 2.47, and 3.84 g oil/g, respectively. HBSS and CASS had higher oil holding ability, which may be related to the absorption of organic matter and chemical compositions. Foaming and foam stability indicate the interfacial properties of surfactant required in formulations containing two insoluble phases (Ma et al., 2018). CASS had the strongest foam capacity (66%) and foam stability (44%) as compared to others. CASS showed the most excellent functional properties among the four polysaccharides for their use in food processing and cosmetics, like milkshakes, and marshmallows (Ji et al., 2019).

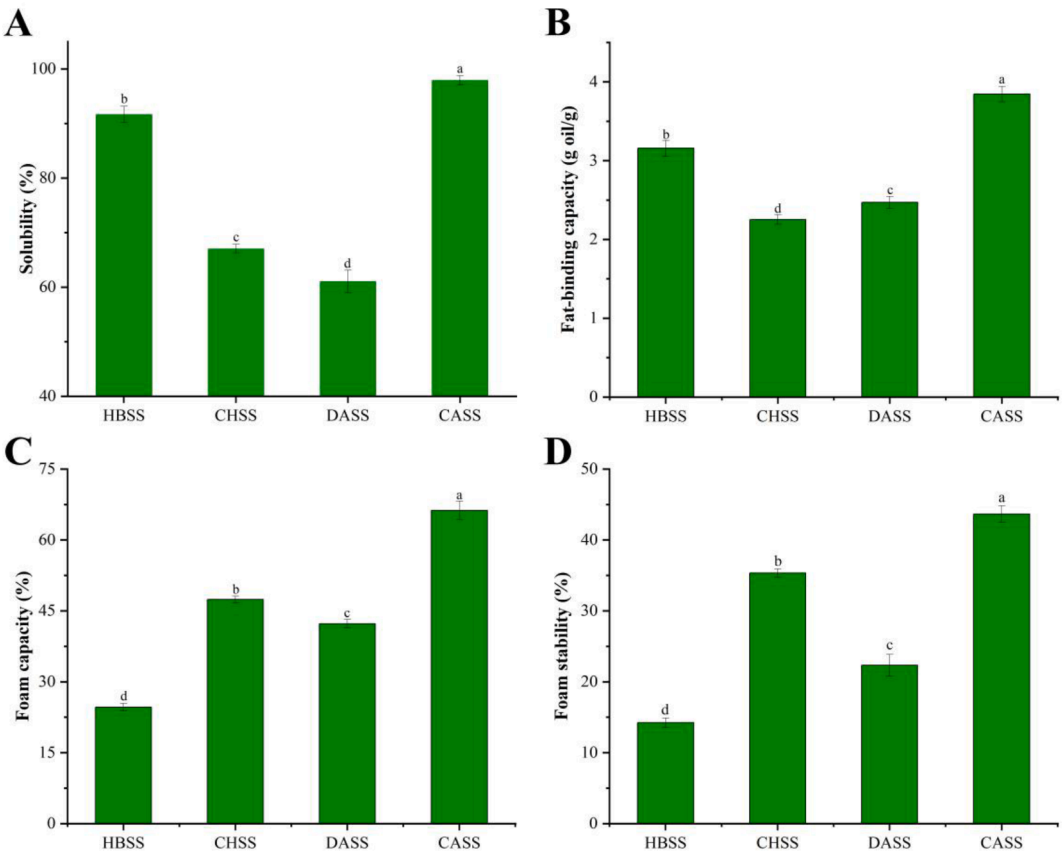

Fig. 4. Solubility, fat-binding capacity, and foam properties of LBSDPs. Values were expressed as mean ± SD of three replicates and different letters indicate significant differences among the different polysaccharides at $p < 0.05$.

Antioxidant activities

ABTS radical scavenging activity

The free radical scavenging capacity of ABTS indicates the oxidative free radical scavenging capacity of antioxidants (Li et al., 2014; Chen et al., 2021). The results of ABTS radical scavenging capacity of HBSS, CHSS, DASS, CASS, and V_C are shown in Fig. 5A. The ABTS free radicals scavenging ability of the four polysaccharides significantly increased with the increasing concentrations of polysaccharides. At 1.0 mg/mL, the clearance rate increased rapidly with the concentration, reaching 71.66%. Further, the concentration continued to increase, and the ABTS free radicals scavenging activity gradually increased, indicating that the ability of CHSS to scavenge ABTS free radicals was limited. At 5 mg/mL, the scavenging capacity of ABTS free radicals was represented as 88.11%, 78.87%, 84.50%, and 95.01%, respectively, which was higher than that of *Amana edulis* polysaccharides (Ji et al., 2019).

DPPH radical scavenging activity

All the four polysaccharides had the DPPH radical scavenging ability in a dose-dependent manner (Fig. 5B) (Vhangani, & Van Wyk, 2013). At 5 mg/mL, the clearance rates of HBSS, CHSS, DASS, and CASS were 59.47%, 62.83%, 76.74%, and 93.74%, respectively. At the same concentration, the order of scavenging ability was CASS > DASS > CHSS > HBSS. At 3 mg/mL, the DPPH radical scavenging ability reached 91.39%, which was close to VC. The difference of DPPH radical scavenging ability among different polysaccharides may be caused by the difference of monosaccharide composition and surface morphological features (Liu et al., 2017).

Fe^{2+} chelating activity

The chelating ability of four polysaccharides showed a typical dose-dependent effect, indicating the increase with the concentration (Fig. 5C). At the same concentration, the order of chelating capacity of the four polysaccharides was as follows: CHSS > DASS > HBSS > CASS. At 5 mg/mL, the Fe^{2+} chelating activity of the four polysaccharides was as follow: 63.10%, 97.70%, 98.36%, and 52.93%, respectively, which was higher than that of *Allium cepa* L. polysaccharides (Ma et al., 2018). At 3 mg/mL, the chelating capacity of CHSS was 93.69%, which was equivalent to the positive control EDTA-2Na.

OH radical scavenging activity

It can be seen from the Fig. 5D that the hydroxyl radical scavenging capacity was dependent on the concentration with the following order: HBSS > CASS > CHSS > DASS, which was similar to the peony seed dreg (Li et al., 2018). At 5 mg/mL, HBSS had the highest scavenging ability up to 70.38%, and CASS, CHSS, and DASS had the similar scavenging capacity such as 48.76%, 48.36%, and 47.77%, respectively.

Total antioxidant activity

Reducing power is an important index to evaluate the antioxidant capacity of substances (Li et al., 2014). The stronger the reducing power indicate the higher antioxidant activity of any substance (Fang, Chen, & Kan, 2020). The reducing power of the four polysaccharides (0–5 mg/mL) can be seen from the Fig. 5E: CASS > DASS > CHSS > HBSS, which was consistent with the results of peony seed dreg (Ji et al., 2019). At (5 mg/mL), the reducing power of CASS was 1.374, which was similar to that of positive control V_C and was slightly higher than that of *Allium cepa* L. and peony seed dreg (Ma et al., 2018, Li et al., 2018).

Conclusion

The continuous extraction method was used to extract polysaccharides from the *L. barbarum* seed dreg. The four polysaccharides had similar UV and IR absorption peaks. Monosaccharide was the main chemical component beside a small amount of protein. All the polysaccharides contained six typical monosaccharides, but there were differences in the content and distribution of monosaccharides. Their molecular weights were 5985, 7062, 5962, and 8762 Da, respectively, and this difference was related to their different antioxidant activity. CASS showed the strongest DPPH radical scavenging ability and reducing power. While, CHSS had the strongest ferrous ions chelating ability, HBSS had the strongest OH radical scavenging ability. In terms of

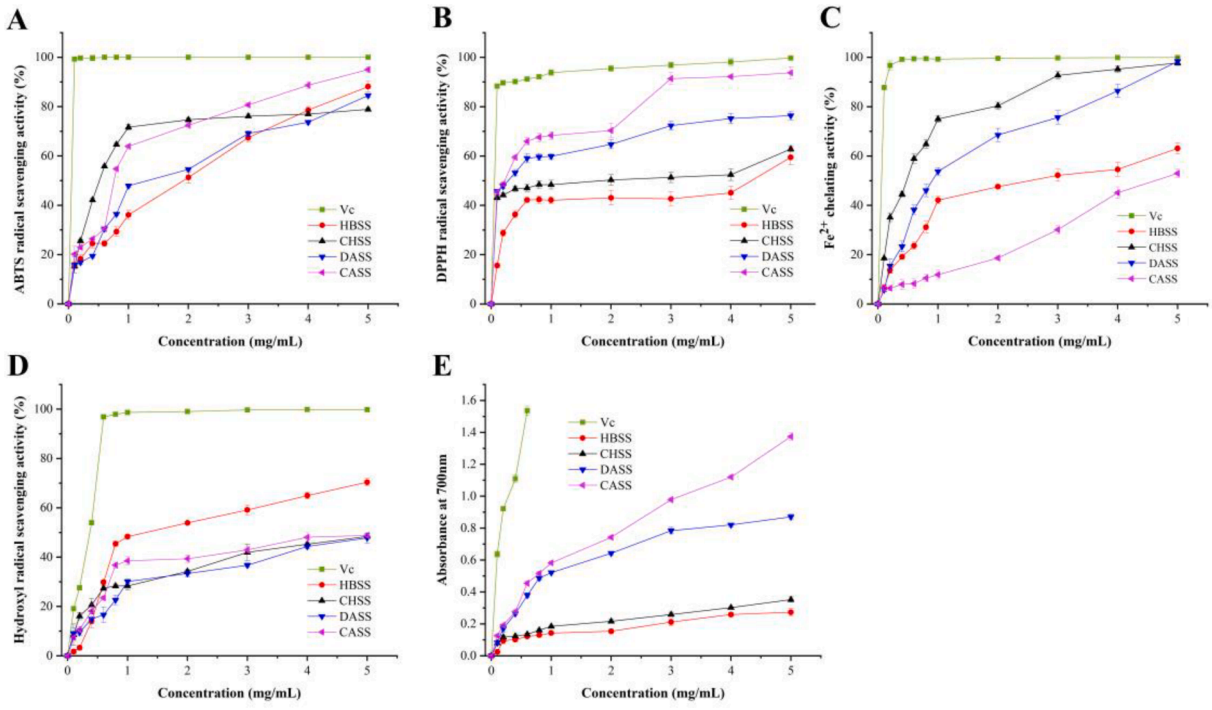

Fig. 5. Antioxidant properties of LBSDPs. (A) ABTS radical scavenging activity of LBSDPs; (B) DPPH radical scavenging activity of LBSDPs; (C) Fe^{2+} chelating ability of LBSDPs; (D) OH radical scavenging activity of LBSDPs; (E) Reducing power of LBSDPs.

functional properties, HBSS and CASS both had better solubility and oil holding capacity. While, CASS and CHSS had better foam capacity and foam stability. Altogether, the polysaccharides continuously extracted from *L. barbarum* seed dreg hold potential prospects in food and cosmetics industry.

Declaration of Competing Interest

The authors declare that they have no known competing financial interests or personal relationships that could have appeared to influence the work reported in this paper.

Acknowledgments

This work was supported by the Key research and development projects in Ningxia Province (2021BEF02013), the Researchers Supporting Project No. (RSP-2021/138) King Saud University (Riyadh, Saudi Arabia), National Natural Science Foundation of Ningxia Province (2021AAC02019), the Youth talent cultivation project of North Minzu University (2021KYQD27, FWNX14), the Major Projects of Science and Technology in Anhui Province (201903a06020021, 202004a06020042, 202004a06020052).

References

Abuduwaili, A., Nuerxiati, R., Mutailifu, P., Gao, Y., Lu, C., & Yili, A. (2022). Isolation structural modification, characterization, and bioactivity of polysaccharides from *Folium Isatidis*. *Industrial Crops & Products, 176*, Article 114319.

Al-Sheraji, S. H., Ismail, A., Manap, M. Y., Mustafa, S., Yusof, R. M., & Hassan, F. A. (2012). Purification, characterization and antioxidant activity of polysaccharides extracted from the fibrous pulp of *Mangifera pajang* fruits. *LWT – Food Science and Technology, 48*, 291–296.

Bellich, B., Elisei, E., Heyd, R., Saboungi, M. L., & Cesàro, A. (2015). Isothermal dehydration of thin films. *Journal of Thermal Analysis and Calorimetry, 121*, 963–973.

Chen, C., Wang, H., Hong, T., Huang, X., Xia, S., Zhang, Y., … Nie, S. (2022). Effects of tea polysaccharides in combination with polyphenols on dextran sodium sulfate-induced colitis in mice. *Food Chemistry: X, 13*, Article 100190.

Chen, X. Y., Sun-Waterhouse, D., Yao, W. Z., Li, X., Zhao, M. M., & You, L. J. (2021). Free radical-mediated degradation of polysaccharides: Mechanism of free radical formation and degradation, influence factors and product properties. *Food Chemistry, 365*, Article 130524.

Cui, C., Lu, J. H., Sun-Waterhouse, D. X., Mu, L. X., Sun, W. Z., Zhao, M. M., & Zhao, H. F. (2016). Polysaccharides from *Laminaria japonica*: Structural characteristics and antioxidant activity. *LWT - Food Science and Technology, 73*, 602–608.

Fang, C. C., Chen, G. G., & Kan, J. Q. (2020). Comparison on characterization and biological activities of *Mentha haplocalyx* polysaccharides at different solvent extractions. *International Journal of Biological Macromolecules, 154*, 916–928.

Hirai, M., Hagiwara, Y., Takeuchi, K., Kimura, R., Onai, T., Kawai-Hirai, R., … Sugiyama, M. (2012). Thermal unfolding and refolding of protein under osmotic pressure clarified by wide-angle X-ray scattering. *Thermochimica Acta, 532*, 15–21.

Iijima, M., Hatakeyama, T., & Hatakeyama, H. (2012). DSC and TMA studies on freezing and thawing gelation of galactomannan polysaccharide. *Thermochimica Acta, 532*, 83–87.

Ji, Y. H., Liao, A. M., Huang, J. H., Thakur, K., Li, X. L., & Wei, Z. J. (2019). Physicochemical and antioxidant potential of polysaccharides sequentially extracted from *Amana edulis*. *International Journal of Biological Macromolecules, 131*, 453–460.

Kan, X. H., Chen, G. J., Zhou, W. T., & Zeng, X. X. (2021). Application of protein-polysaccharide Maillard conjugates as emulsifiers: Source, preparation and functional properties. *Food Research International, 150*, Article 110740.

Kulczyński, B., & Gramza-Michałowska, A. (2016). Goji Berry (*Lycium barbarum*): Composition and Health Effects – a Review. *Polish Journal of Food and Nutrition Sciences, 66*, 67–75.

Li, C., Fu, X., Huang, Q., Luo, F. X., & You, L. J. (2014). Ultrasonic extraction and structural identification of polysaccharides from *Prunella vulgaris* and its antioxidant and antiproliferative activities. *European Food Research and Technology, 240*, 49–60.

Li, G. L., Shi, J. Y., Suo, Y. R., Sun, Z. W., Xia, L., Zheng, J., … Liu, Y. J. (2011). Supercritical CO_2 cell breaking extraction of *Lycium barbarum* seed oil and determination of its chemical composition by HPLC/APCI/MS and antioxidant activity. *LWT - Food Science and Technology, 44*, 1172–1178.

Li, H., Wang, X., Xiong, Q., Yu, Y., & Peng, L. C. (2020). Sulfated modification, characterization, and potential bioactivities of polysaccharide from the fruiting bodies of *Russula virescens*. *International Journal of Biological Macromolecules, 154*, 1438–1447.

Li, J., Chang, M. M., Zhou, X. M., Li, D. P., & Li, Y. X. (2014). Facile synthesis of gold nanopuncheons with high-index facets and their SERS effects on Rhodamine 6G. *Materials Research Bulletin, 59*, 150–153.

Li, X. L., Thakur, K., Zhang, Y. Y., Tu, X. F., Zhang, Y. S., Zhu, D. Y., … Wei, Z. J. (2018). Effects of different chemical modifications on the antibacterial activities of polysaccharides sequentially extracted from peony seed dreg. *International Journal of Biological Macromolecules, 116*, 664–675.

Liu, X. X., Ning, Z. M., Zuo, Z. C., Wang, P., Yin, R. H., Gao, N., … Zhao, J. H. (2022). The glycosidic bond cleavage and desulfation investigation of fucosylated glycosaminoglycan during mild acid hydrolysis through structural analysis of the resulting oligosaccharides. *Carbohydrate Research, 511*, Article 108493.

Liu, X. Y., Chen, Y. X., Wu, L. X., Wu, X. Q., Huang, Y. F., & Liu, B. (2017). Optimization of polysaccharides extraction from *Dictyophora indusiata* and determination of its antioxidant activity. *International Journal of Biological Macromolecules, 103*, 175–181.

Long, X. Y., Yan, Q., Cai, L. J., Li, G. Y., & Luo, X. G. (2020). Box-Behnken design-based optimization for deproteinization of crude polysaccharides in *Lycium barbarum* berry residue using the Sevag method. *Heliyon, 6*, Article e03888.

Luo, A. X., He, X. J., Zhou, S. D., Fan, Y. J., Luo, A. S., & Chun, Z. (2010). Purification, composition analysis and antioxidant activity of the polysaccharides from *Dendrobium nobile* Lindl. *Carbohydrate Polymers, 79*, 1014–1019.

Ma, Y. L., Zhu, D. Y., Thakur, K., Wang, C. H., Wang, H., Ren, Y. F., … Wei, Z. J. (2018). Antioxidant and antibacterial evaluation of polysaccharides sequentially extracted from onion (*Allium cepa* L.). *International Journal of Biological Macromolecules, 111*, 92–101.

Mascia, A., Carradorib, S., Casadeic, M. A., Paolicellic, P., Petralitoc, S., Ragnoc, R., & Cesa, S. (2018). *Lycium barbarum* polysaccharides: Extraction, purification, structural characterisation and evidence about hypoglycaemic and hypolipidaemic effects. A review. *Food Chemistry, 254*, 377–389.

Sengkhamparn, N., Verhoef, R., Schols, H. A., Sajjaanantakul, T., & Voragen, A. G. (2009). Characterisation of cell wall polysaccharides from okra (*Abelmoschus esculentus* (L.) Moench). *Carbohydrate Research, 344*, 1824–1832.

Tan, M. H., Zhao, Q. S., & Zhao, B. (2021). Physicochemical properties, structural characterization and biological activities of polysaccharides from quinoa (*Chenopodium quinoa* Willd.) seeds. *International Journal of Biological Macromolecules, 193*, 1635–1644.

Tang, W., Liu, C. C., Liu, J. J., Hu, L. Y., Huang, Y. S., Yuan, L., … Nie, S. P. (2020). Purification of polysaccharide from *Lentinus edodes* water extract by membrane separation and its chemical composition and structure characterization. *Food Hydrocolloids, 105*, Article 105851.

Vhangani, L. N., & Van Wyk, J. (2013). Antioxidant activity of Maillard reaction products (MRPs) derived from fructose-lysine and ribose-lysine model systems. *Food Chemistry, 137*, 92–98.

Wang, X. Q., Zhang, M. L., Zhang, D. W., Wang, X. L., Cao, H. J., Zhang, Q., & Yan, C. Y. (2019). Structural elucidation and anti-osteoporosis activities of polysaccharides obtained from *Curculigo orchioides*. *Carbohydrate Polymers, 203*, 292–301.

Wang, Y., Han, Q. Q., Bai, F., Luo, Q., Wu, M. L., Song, G., … Wang, Y. Q. (2020). The assembly and antitumor activity of lycium barbarum polysaccharide-platinum-based conjugates. *Journal of Inorganic Biochemistry, 205*, Article 111001.

Xie, H., Fang, J., Farag, M. A., Li, Z., Sun, P., & Shao, P. (2022). Dendrobium officinale leaf polysaccharides regulation of immune response and gut microbiota composition in cyclophosphamide-treated mice. *Food Chemistry: X, 13*, Article 100235.

Xie, J. H., Jin, M. L., Morris, G. A., Zha, X. Q., Chen, H. Q., Yi, Y., … Xie, M. Y. (2016). Advances on bioactive polysaccharides from medicinal plants. *Critical Reviews in Food Science and Nutrition, 56*, 60–84.

Xu, G. Y., Liao, A. M., Huang, J. H., Zhang, J. G., Thakur, K., & Wei, Z. J. (2019). Evaluation of structural, functional, and anti-oxidant potential of differentially extracted polysaccharides from potatoes peels. *International Journal of Biological Macromolecules, 129*, 778–785.

Yang, Y., Chang, Y. F., Wu, Y., Liu, H. R., Liu, Q. S., Kang, Z. Z., … Duan, J. Y. (2021). A homogeneous polysaccharide from *Lycium barbarum*: Structural characterizations, anti-obesity effects and impacts on gut microbiota. *International Journal of Biological Macromolecules, 183*, 2074–2087.

Yu, Y., Shen, M. Y., Song, Q. Q., & Xie, J. H. (2018). Biological activities and pharmaceutical applications of polysaccharide from natural resources: A review. *Carbohydrate Polymers, 183*, 91–101.

Yuan, E., Nie, S., Liu, L., & Ren, J. (2021). Study on the interaction of *Hericium erinaceus* mycelium polysaccharides and its degradation products with food additive silica nanoparticles. *Food Chemistry: X, 12*, Article 100172.

Yuan, Q. H., Xie, F., Tan, J., Yuan, Y., Mei, H., Zheng, Y., & Sheng, R. (2022). Extraction, structure and pharmacological effects of the polysaccharides from *Cordyceps sinensis*: A review. *Journal of Functional Foods, 89*, Article 104909.

Zheng, Y., Pang, X., Zhu, X. X., Meng, Z. Y., Chen, X. J., Zhang, J., … Ma, B. P. (2021). *Lycium barbarum* mitigates radiation injury via regulation of the immune function, gut microbiota, and related metabolites. *Biomedicine & Pharmacotherapy, 139*, Article 111654.